Communication

Identification of the Nitrogen Donor Hydrogen Bonded with the Semiquinone at the Q Site of the Cytochrome *bo* from *Escherichia coli*

Myat T. Lin, Rimma I. Samoilova, Robert B. Gennis, and Sergei A. Dikanov

J. Am. Chem. Soc., **2008**, 130 (47), 15768-15769 • DOI: 10.1021/ja805906a • Publication Date (Web): 05 November 2008

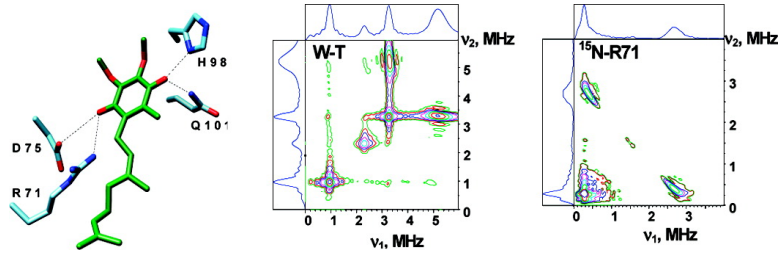

More About This Article

Additional resources and features associated with this article are available within the HTML version:

- Supporting Information
- Access to high resolution figures
- Links to articles and content related to this article
- Copyright permission to reproduce figures and/or text from this article

View the Full Text HTML

J|A|C|S
COMMUNICATIONS

Published on Web 11/05/2008

Identification of the Nitrogen Donor Hydrogen Bonded with the Semiquinone at the Q_H Site of the Cytochrome *bo*$_3$ from *Escherichia coli*

Myat T. Lin,[†] Rimma I. Samoilova,[||] Robert B. Gennis,*[,‡] and Sergei A. Dikanov*[,§]

Departments of Biophysics and Computational Biology, Biochemistry, and Veterinary Clinical Medicine, University of Illinois at Urbana−Champaign, Urbana, Illinois 61801, and Institute of Chemical Kinetics and Combustion, Russian Academy of Sciences, Novosibirsk 630090, Russia

Received July 28, 2008; E-mail: dikanov@illinois.edu

E. coli cytochrome (cyt) *bo*$_3$ ubiquinol oxidase catalyzes the two-electron oxidation of ubiquinol and the four-electron reduction of O_2 to water. The enzyme contains three redox-active metal centers: a low spin heme *b*, which is involved in quinol oxidation, and the heme o_3/Cu_B bimetallic center, which is the site where O_2 binds and is reduced to water. The ubiquinol oxidation occurs with a semiquinone (SQ) intermediate in an overall reaction that releases two protons to the periplasm. The enzyme contains two Q sites:[1−6] a low affinity site (Q_L), which is equilibrated with the quinone pool in the membrane and functions as the substrate (QH_2) binding site, and a high affinity (Q_H) site, from which Q is not readily removed and which stabilizes a SQ.[7−10] The Q_H site quinone appears to function as a tightly bound cofactor, similar to the Q_A site of the reaction centers. The X-ray structure of cyt *bo*$_3$[11] does not contain any bound quinone, but mutational substitutions of R71, D75, H98, and Q101 modulate the properties of the Q_H site, forming the basis of a model of the Q_H binding site (see Supporting Information).[2−4,11]

The interaction of the SQ with the protein environment in cyt *bo*$_3$ has been studied by pulsed EPR spectroscopy. X-band ESEEM data show that there is one H-bond to the Q_H SQ from a nitrogen donor.[5,6,12,13] The speculated identification of this nitrogen has been based on the quadrupole coupling constant (qcc) determined from the ESEEM spectra.[5,6,12,13] Its value, $K = e^2qQ/4h = 0.93$ MHz, most closely corresponds to the nitrogen from an NH or NH_2 group.[12,13] This value is ∼10% larger than the qcc for the peptide amide nitrogen and significantly exceeds the qcc of the protonated nitrogens in histidine. Hence, the most likely candidates for the H-bond donor are the nitrogens from the side chains of R71 or Q101, though a peptide backbone nitrogen cannot be ruled out completely.

To overcome the existing uncertainties and to identify directly the H-bonded nitrogen, we employed ^{15}N selective labeling in different residues. Proteins were labeled as follows: (1) ^{15}N uniformly labeled Arg; (2) ^{15}N uniformly labeled His; (3) Gln with ^{15}N only in the N_ε position; (4) Arg with ^{15}N only in the two N_η positions; (5) Arg with ^{15}N only in the peptide nitrogen (Scheme 1). The ^{15}N labeling procedures, the preparation of EPR samples, and generation of the SQ are described in Supporting Information. To resolve the interaction of the SQ with ^{14}N and ^{15}N nitrogens we used X-band three-pulse ESEEM and 2D ESEEM (HYSCORE).

The X-band three-pulse ^{14}N ESEEM spectrum of the SQ in wild-type cyt *bo*$_3$ has been described in detail previously.[5,6,12,13] It consists of three intensive narrow lines: $\nu_o = 0.95$ MHz, $\nu_- = 2.32$ MHz, and $\nu_+ = 3.27$ MHz, where $\nu_+ = \nu_o + \nu_-$. There is also a

Scheme 1

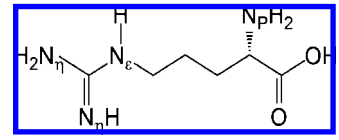

less intensive and broader line at frequency $\nu_{dq} \approx 5.1-5.2$ MHz (see Supporting Information). This spectrum is typical for a single ^{14}N at near cancelation conditions ($|\nu_N - A/2| \approx 0$; ν_N, ^{14}N Zeeman frequency, ∼1.07 MHz in X-band; *A*, hyperfine coupling). The narrow peaks are assigned to the three nuclear quadrupole resonance frequencies, and the broader line is the frequency of the double-quantum transition ν_{dq} from the opposite manifold. The spectroscopic parameters determine the qcc $K = 0.93$ MHz, the asymmetry parameter $\eta = 0.51$, and the hyperfine coupling $A = 1.8$ MHz for this nitrogen.[5,6,12,13] The corresponding HYSCORE spectrum of the SQ in wild-type *bo*$_3$ (Figure 1a) exhibits cross-peaks correlating ν_o, ν_-, and ν_+ with ν_{dq}, thus indicating that they belong to different manifolds. The most intensive cross-peaks in Figure 1a are from the (ν_+,ν_{dq}) correlations. There are also three intensive peaks at the diagonal points corresponding to ν_o, ν_-, and ν_+.

Specifically, the ^{15}N-labeled proteins were examined to identify the nitrogen responsible for the ^{14}N features observed with wild-type protein. It is assumed that only R71, Q101, and H98 are significant in interpreting the results from ^{15}N-labeled Arg, Gln, and His residues, respectively. Figure 1b shows the spectrum of *bo*$_3$ with ^{15}N-labeled N_η in R71. In addition to the unchanged ^{14}N features, this spectrum resolves two new weak cross-peaks from ^{15}N centered around a diagonal point with a ^{15}N Zeeman frequency $^{15}\nu_N$ ∼1.5 MHz with coordinates (1.58, 1.43) MHz corresponding to the hyperfine coupling $^{15}A = 0.15$ MHz. The spectrum of the *bo*$_3$ with ^{15}N labeled N_p of R71 did not show any resolved peaks from ^{15}N. A peak of very low intensity located at the diagonal point ($^{15}\nu_N$,$^{15}\nu_N$) was observed for the *bo*$_3$ with labeled N_ε of Q101, thus indicating very weak dipolar interaction between the unpaired electron and a distant ^{15}N nucleus. The spectrum of the *bo*$_3$ with uniformly ^{15}N-labeled H98 (Figure 1c) also shows the peak with a maximum at the diagonal point ($^{15}\nu_N$,$^{15}\nu_N$). However, it is accompanied by extended shoulders with weakly resolved maxima corresponding to couplings of ∼0.3 and 0.6 MHz. This line can be produced by interactions with up to three ^{15}N's, and more specific labeling will be needed to resolve the exact coupling from each nitrogen of this residue. The spectra of these samples have clearly shown that labeled nitrogens in each of the residues R71 (except N_p), Q101, and H98 are located in close proximity of the paramagnetic SQ, and some of them even carry a small fraction of the unpaired spin density producing isotropic hyperfine splittings of ∼0.1 to 0.6 MHz. However, none of these ^{15}N-labeled positions

[†] Biophysics and Computational Biology, University of Illinois at Urbana−Champaign.
[‡] Biochemistry, University of Illinois at Urbana−Champaign.
[§] Veterinary Clinical Medicine, University of Illinois at Urbana−Champaign.
[||] Russian Academy of Sciences.

10.1021/ja805906a CCC: $40.75

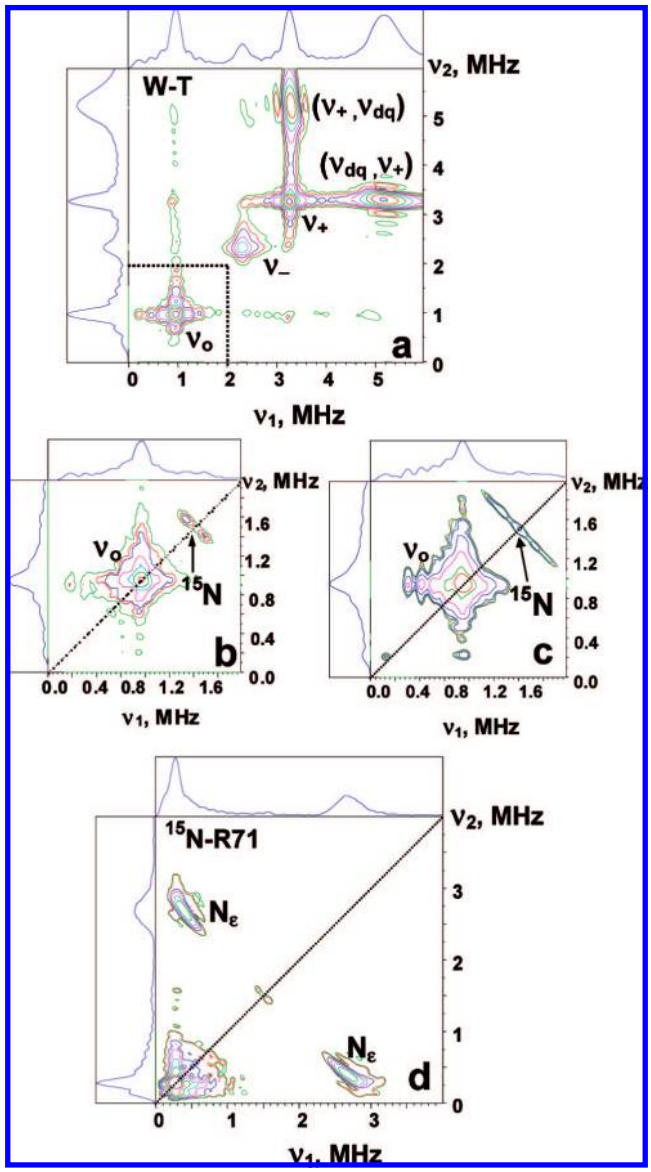

Figure 1. ^{14}N and/or ^{15}N HYSCORE spectra in contour presentation of the SQ in the Q_H-site of the wild-type bo_3 oxidase (a), bo_3 with ^{15}N labeled N_ηs in R71 (b), uniformly ^{15}N-labeled H98 (c), and uniformly ^{15}N-labeled R71 (d). Magnetic field, time τ, and microwave frequency, respectively: 345.0 mT, 136 ns, 9.70 GHz (a); 346.3 mT, 136 ns, 9.712 GHz (b); 346.3 mT, 200 ns, 9.712 GHz (c); 345.9 mT, 136 ns, 9.71 GHz (d).

is responsible for the X-band ^{14}N ESEEM features of the wild-type protein which would result in a significantly larger ^{15}N hyperfine coupling, $^{15}A \sim 2.5$ MHz (recalculated from $A \sim 1.8$ MHz for ^{14}N).

A dramatic change of the ESEEM spectra, accompanied by the complete disappearance of the ^{14}N peaks, is observed in the bo_3 with uniformly ^{15}N-labeled R71 (Figure 1d). The HYSCORE spectrum of the SQ in this protein contains two intense cross-peaks ($\mathbf{N}_\varepsilon$) from ^{15}N with a maximum at (2.74, 0.34) MHz corresponding to the coupling $^{15}A = 2.4$ MHz, as well as weak features similar to ones observed for R71 with $^{15}N_\eta$'s (Figure 1b). The extended shape of the $\mathbf{N}_\varepsilon$ peaks results from the anisotropic hyperfine interaction with the average perpendicular component of the tensor $T \sim 0.4$ MHz. Taking into account that R71, selectively labeled in the N_η and N_p positions, does not result in features correlating to a large hyperfine coupling, it can be definitively concluded that the N_ε of R71 is a H-bond donor to the carbonyl oxygen of the SQ. The unpaired spin density fraction of $\sim 1.2 \times 10^{-3}$ is transferred onto the N_ε nucleus through the H-bond bridge (see Supporting Information). Spin density delocalization continues further through N_ε and reaches at least one N_η, which is separated by two bonds from the N_ε in the side chain, producing the resolved coupling $^{15}A \sim 0.15$ MHz.

These experiments also provide evidence that some unpaired spin density (^{15}A coupling up to 0.6 MHz) is transferred to the nitrogens of H98, suggesting its involvement in an H-bond with a larger O−H bond distance or with a less favorable configuration of the spin density transfer than the H-bond with the N_ε of R71. The weakly coupled nitrogens with $^{15}A < 0.6$ MHz ($^{14}A < 0.43$ MHz) are far away from the cancelation condition and, as a result, do not produce resolved contributions to the X-band 1D and 2D ^{14}N ESEEM spectra. The evidence also supports a weak interaction of the SQ with the side chain nitrogen of Q101.

In summary, the experiments with the Q_H site SQ in the series of selectively ^{15}N labeled bo_3 oxidases have directly identified the N_ε of R71 as the H-bond donor responsible for the features observed in the X-band ^{14}N ESEEM of wild-type bo_3. In addition, selective ^{15}N labeling has allowed us for the first time to probe a distribution of the unpaired spin density on the side-chain nitrogens from the residues around the SQ in the quinone binding site. These results form a basis for more advanced theoretical analysis of the protein−SQ interaction in the Q_H site, using the model of the neutral radical indicated by the proton hyperfine couplings,[12,13] in conjunction with other available magnetic resonance data.[14]

Acknowledgment. This investigation was supported by the NIH GM062954 grant (S.A.D.) and DE-FG02-08ER15960 (S.A.D.) and DE-FG02-87ER13716 (R.B.G.) grants from Chemical Sciences, Geosciences and Biosciences Division, Office of Basic Energy Sciences, Office of Sciences, U.S. DOE, and NCRR/NIH Grant S10-RR15878 for instrumentation.

Supporting Information Available: ^{15}N labeling procedures, preparation of EPR samples, three-pulse and HYSCORE spectra, model of the Q_H-site, spin density transfer. This material is available free of charge via the Internet at http://pubs.acs.org.

References

(1) Tsubaki, M.; Hori, H.; Mogi, T. *J. Inorg. Biochem.* **2000**, *82*, 19–25.
(2) Hellwig, P.; Yano, T.; Ohnishi, T.; Gennis, R. B. *Biochemistry* **2002**, *41*, 10675–10679.
(3) Hellwig, P.; Barquera, B.; Gennis, R. B. *Biochemistry* **2001**, *40*, 1077–1082.
(4) Hellwig, P.; Mogi, T.; Tomson, F. L.; Gennis, R. B.; Iwata, J.; Miyoshi, H.; Mantele, W. *Biochemistry* **1999**, *38*, 14683–14689.
(5) Grimaldi, S.; MacMillan, F.; Ostermann, T.; Ludwig, B.; Michel, H.; Prisner, T. *Biochemistry* **2001**, *40*, 1037–1043.
(6) Grimaldi, S.; Ostermann, T.; Weiden, N.; Mogi, T.; Miyoshi, H.; Ludwig, B.; Michel, H.; Prisner, T.; MacMillan, F. *Biochemistry* **2003**, *42*, 5632–5639.
(7) Puustinen, A.; Verkhovsky, M. I.; Morgan, J. E.; Belevich, N. P.; Wikström, M. *Proc. Natl. Acad. Sci. U.S.A.* **1996**, *93*, 1545–1548.
(8) Mogi, T.; Sato-Watanabe, M.; Miyoshi, H.; Orii, Y. *FEBS Lett.* **1999**, *457*, 223–226.
(9) Musser, S. M.; Stowell, M. H. B.; Lee, H. K.; Rumbley, J. N.; Chan, S. I. *Biochemistry* **1997**, *36*, 894–902.
(10) Schultz, B. E.; Edmondson, D. E.; Chan, S. I. *Biochemistry* **1998**, *37*, 4160–4168.
(11) Abramson, J.; Riistama, S.; Larsson, G.; Jasaitis, A.; Svensson-Ek, M.; Laakkonen, L.; Puustinen, A.; Iwata, S.; Wikström, M. *Nat. Struct. Biol.* **2000**, *7*, 910–917.
(12) Yap, L. L.; Samoilova, R. I.; Gennis, R. B.; Dikanov, S. A. *J. Biol. Chem.* **2006**, *281*, 16879–16887.
(13) Yap, L. L.; Samoilova, R. I.; Gennis, R. B.; Dikanov, S. A. *J. Biol. Chem.* **2007**, *282*, 8777–8785.
(14) Kasprzak, S.; Kaupp, M.; MacMillan, F. *J. Am. Chem. Soc.* **2006**, *128*, 5661–5671.

JA805906A